American Journal of Energy Research, 2016, Vol. 4, No. 2, 27-34
Available online at http://pubs.sciepub.com/ajer/4/2/1

DOI:10.12691/ajer-4-2-1

Experimental Investigation of Mass Transfer in a Channel of Contacting Conditioner

I. M. Kuzmenko*, O. V. Makarchuk

Heat-and-Power Engineering Department, NTUU "Kyiv polytechnic institute", Kyiv, Ukraine
*Corresponding author: ozirno@ukr.net

Abstract Mass transfer coefficient for contacting conditioning is determined experimentally and theoretically for steady air. Contribution of diffusion and convection component into mass transfer is estimated. The assessment showed that the contribution of the convection component into mass transfer can be neglected. Thickness of diffusional mass transfer layer was experimentally measured and it less than the theoretical values of displacement layer thickness till 10 times. Therefore the experimental value of mass transfer coefficient exceeds by one order the theoretically calculated ones. The criteria equation is recommended for calculation of mass transfer coefficient at steady air flow in a channel.

Keywords: *mass transfer, contacting conditioner, displacement layer, water film*

Cite This Article: I. M. Kuzmenko, and O. V. Makarchuk, "Experimental Investigation of Mass Transfer in a Channel of Contacting Conditioner." *American Journal of Energy Research*, vol. 4, no. 2 (2016): 27-34. doi: 10.12691/ajer-4-2-1.

1. Introduction

Distinction of the mass transfer process in a contacting conditioner is that air cooling is simultaneous with air humidification and water heating when the temperature of water is higher than condensing point temperature and lower that the temperature of a wet thermometer.

Process takes place in hot air-cold water environment and since water temperature is lower than one of a wet thermometer $t_3 < t_{wb}$, water heating by temperature difference of air and water happens $t_2 - t_3$. Therefore, heat transfers from air to water. Thus, part of the heat goes into water evaporation because of the difference in partial pressures $p_3 - p_2$, conditioned by the difference in air humidity near the water and general layer of air. Let's describe mass transfer in this mode, set the values of the mass transfer coefficients and obtain the empirical equation for process calculation.

The heat and mass transfer processes require calculation of the evaporative cooling of water film. These depend on the water film and air velocities, contact area and the input temperatures.

There are four types of models for calculating of the heat and mass transfer processes at evaporative cooling.

The first group is based on the liquid heat balance equation with substitution of Lewis number $Le = \alpha / \beta / c = 1$ (Merkel's equation) [1,2]

$$G_3 c_3 \Delta t_3 = G_2 \Delta h_2 = \beta (h_s - h_w) \Delta f . \quad (1)$$

Equation (1) illustrates the temperature of water film depend on mass transfer between air and water film and gives good results at wet-bulb water temperature ($Le = 1$).

The next type of models is based on the calculation of heat flow to water film by heat and mass transfer coefficients to air [3,4]. Next equations describe evaporative cooling of water film.

Heat balance of water film

$$G_3 c_3 \Delta t_3 = Q_\alpha + Q_\beta , \quad (2)$$

where heat transfer at cooling

$$Q_\alpha = \alpha (t_w - t_s) f \quad (3)$$

and mass transfer at evaporation

$$Q_\beta = r \beta (p_w - p_s) f . \quad (4)$$

The model uses the known values of heat and mass transfer coefficients and gives the output temperatures of the component, partial pressure of vapour.

Another type of models uses system of differential equations describes the evaporative cooling of water film at countercurrent flow [5,6].

Energy equation for water film and air and also compensation equation for air are numerically solved taking in account the experimental coefficient values for heat and mass transfer.

The model (2-4) was modified by reducing of the water film thickness [7,8]. But this increased the deviation of theoretical and experimental result.

Another group of models is based on the numerical study of system continuity, momentum, energy and concentration equations for air and water film [9,10,11,12] at concurrent water-air flow.

Heat balance on the border between the water film and air

$$q_3 = \left[\lambda \frac{\partial t}{\partial R} \right]_3 + \dot{m} r \quad (5)$$

allows us to define the Nusselt number and heat transfer coefficient between water film and air film

$$Nu = \frac{h(2R)}{\lambda_3} = \frac{q(2R)}{\lambda_3(\Delta t)}. \quad (6)$$

Similarly, mass transfer coefficient is defined from the Sherwood number:

$$Sh = \frac{h(2R)}{D} = \frac{\dot{m}(1-\omega)(2R)}{\rho_2 D(\Delta\omega)}. \quad (7)$$

This group of models (5-7) allows calculating values of the heat and mass transfer coefficients, but deviation between numerical and experimental results for this group of models is up to 33 %.

There are some disadvantages of the methods described above. The experimental value of the heat and mass transfer coefficients gives a variety of output temperatures and a partial pressure of vapour in the air. The analytical calculation does not need an experimental value of heat and mass transfer but this method gives a substantial error. The Lewis analogy for determining of mass transfer coefficient can be fulfilled or not. So the objective of the paper is an investigation of principles of calculation of mass transfer coefficient in a contact conditioner. The following tasks are performed:

– values of the diffusion and convection mass transfer is calculated experimentally and checked by theory. The comparison of value of diffusion and convection mass transfer is performed;

– coefficient of diffusion mass transfer is investigated from the boundary layer theory. The experimental results were compared with simulation results;

– using the similarity theory, generalized experimental results of mass transfer in a channel of a contact conditioner.

2. Theory of Mass Transfer Process

Let's assume that the mass transfer process is carried out by diffusion as an analog to heat conduction and convection, since there is no analog to emission for mass transfer on molecular level. We will discuss the combination of diffusional and convectional mass transfer below [13]. On the bottom of the glass tube there's water (Figure 1) and over the open end there's an air flow with a certain mass fraction of vapor ω_{1s}.

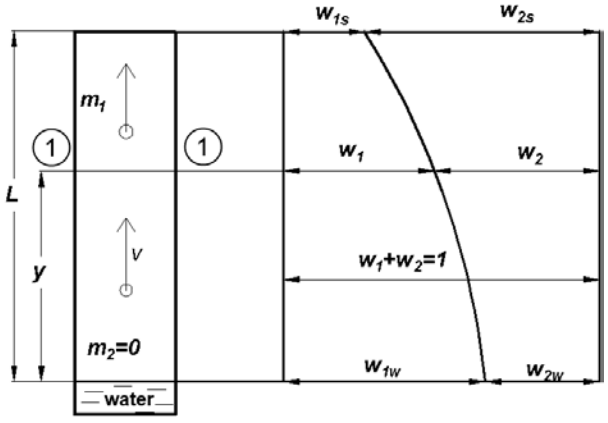

Figure 1. Diffusional and convectional mass transfer

Pressure in the tube is constant and equal to the exterior pressure. Let's assume that temperature in the tube is constant and mass fraction ω_{1s} of vapor out of the tube and on the water's surface differ.

Vapor's partial pressure out of the tube and on the water's surface also differs. Vapor's partial pressure on the water's surface is equal to the saturation pressure for the water's temperature. Mass fraction ω_{1s} represents the saturated steams for the water's temperature.

In the tube there's a mass fraction gradient ω_1 and a diffusional water vapor flow, according to the Fick's law.

Since vapor's mass fraction ω_1 and air's together equal one, mass fraction gradient of vapor is equal to the mass fraction gradient of air $\omega_1 + \omega_2 = (m_1 + m_2)/m = 1$. This means that together with a vapor flow also exists an air flow in the opposite direction. Diffusion of such air also corresponds with the Fick's law. However the bottom part of the tube doesn't have a hole. Therefore to compensate the diffusional descending air flow the tube has to have a convectional ascending flow.

Let's assume that the velocity of this convectional flow equals υ. And the amount of vapor moved by the flow from one unit of area of the tube 1-1 after one unit of time is $\rho_1\upsilon$. This means that the general vapor mass velocity through a section 1-1 is described by the following equation

$$m_1 = -\rho D\frac{d\omega_1}{dy} + \rho_1\upsilon_1. \quad (8)$$

Similar equation is true for air flow. But, since this flow equals zero, we have a following equation

$$m_2 = -\rho D\frac{d\omega_2}{dy} + \rho_2\upsilon_2 = 0. \quad (9)$$

From here we get air's velocity

$$\upsilon_2 = \frac{D}{\omega_2}\cdot\frac{d\omega_2}{dy}. \quad (10)$$

Mass fraction of vapor in air we'll write as $\omega_2 = 1-\omega_1$; $\frac{d\omega_2}{dy} = -\frac{d\omega_1}{dy}$. As result we have vapor velocity that flowing from water film and equal velocity of convectional air $\upsilon = \upsilon_1 = \upsilon_2$ because the vapor is created the same air flow

$$\upsilon = -\frac{D}{1-\omega_1}\frac{d\omega_1}{dy}. \quad (11)$$

Then, taking notice that $\rho + \frac{\rho_1}{1-\omega_1} = \frac{\rho^2 - \rho\rho_1 + \rho\rho_1}{\rho - \rho_1} = \frac{\rho^2}{\rho_2}$ vapor's mass fraction flow through the tube, according the equation (8), is the following

$$m_1 = -\rho D\frac{d\omega_1}{dy} - \frac{\rho_1}{1-\omega_1}D\frac{d\omega_1}{dy} = -\frac{\rho^2}{\rho^2}D\frac{d\omega_1}{dy}.$$

If the result of the equation (11) is put into eq. (8), we receive

$$m_1 = -\rho D \frac{d\omega_1}{dy} + \rho_1 \upsilon = \rho(1-\omega_1)\upsilon + \rho_1 \upsilon = \rho \upsilon \quad (12)$$

as $\rho \upsilon \omega_1 = \frac{m}{V}\frac{m_1}{m}\upsilon = \rho_1 \upsilon$.

Let's test experimentally the dependencies (1-5) on a experimental unit in a mode that simulates the flow in a channel of a contacting conditioner.

3. Description of the Experimental Facility

An experimental facility was build for research purposes (Figure 2). Experiments take place in a state of countercurrent flows of heat carriers – water film (tap water was used) and air. The experimental unit allowed the input of heat carriers with specified losses and parameters.

The main element of the experimental unit is the work area – regular wire net filled channel. Losses on the unit are regulated by variable-area flowmeter (4, 5) and the input temperatures – by powerful electric water and air heaters (2, 3). The facility's supply lines are made from standard tubes, sealed by screw joints. In order to decrease the losses in water and air heaters, supply lines for hot heat carriers and the work area (1) are isolated by asbestine cord lines.

Experimental unit (1), shown on Figure 2 (to the right), is 1 m high and ∅ 16.5 mm. Water, after going through the electric heater (3), thanks to the design of the overflow type filler (6), is equally distributed on the exterior area of the tube with a wire net (7). The latter is constructed by contact welding of stainless steel to a ∅ 16 mm tube from stainless steel too. Width of the wire net was selected so that in place of welding edges of the wire net was back to back. Before the experiments the wire net was degreased with ethanol. Tube with the wire net (7) filler (6) and water collector (9) were assembled still inside a glass tube (8), with an interior ∅ 37 mm. For consolidating the tube with metal areas rubber stuffing boxes were used. The input and output air temperatures in the experimental unit (8) is taken by thermocouples I, III. Input water film temperature in the experimental unit is taken before the filler 6 (thermocouple IV), and output water film temperature was taken directly in the collector 9 (thermocouple II). During montage of the unit vertical positioning of the experimental unit was controlled, and after it the working capacity of heat carrier losses and heat losses were tested.

Experimental researches were conducted on a tube with a wire net, 2χ =16,5 mm, 1000 mm in height with the input air temperature t_{2in} = 80...150°C, input water film temperature t_{3in} = 23 C, with air velocity W = 1,6...5,7 m/s and water concentration G_3 / L = 0,07 kg/ms.

During the experimental researches that were conducted by a classic plan and consisted in increasing air flow rate with constant air and water film input temperatures, these parameters were measured:

- air and water flow rate – by variable-area flowmeters,
- water film and air input and output temperature (temperature was taken by thermocouples ∅ 0.5 mm),
- by hygrometer – absolute input air humidity (output air humidity is calculated from the heat balance equation).

Results of the experimental research are shown in Table 1.

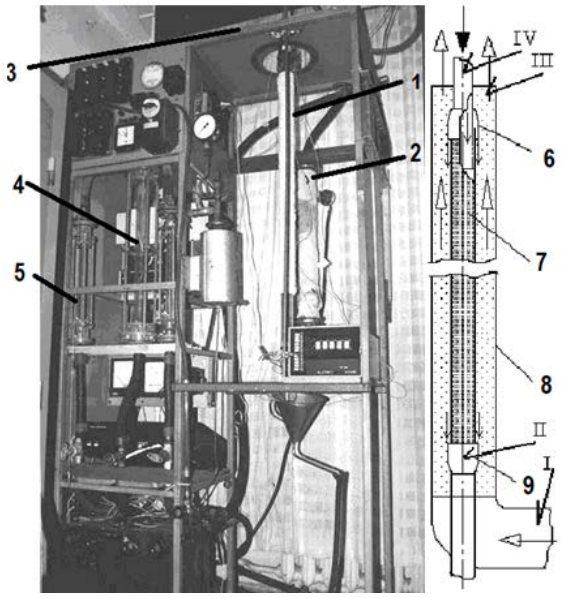

Figure 2. Experimental facility (on the left) and drawing of the experimental unit: 1 – experimental unit, 2 – electric air heater, 3 – electric water heater, 4 – water variable-area flowmeters, 5 – air variable-area flowmeters, 6 – filler, 7- tube with a wire net, 8 – glass tube, 9 – collector, I-IV – thermocouple.

Table 1. The results of experiment

N	G_3, kg/h	G_2, m^3/h	t_{2in}, °C	t_{2out}, °C	t_{3in}, °C	t_{3out}, °C
1	13	6.15	80.2	37.2	23	25
2	13	6.15	80	37	23	25
3	13	12.37	80	42.4	23.2	26.4
4	13	12.37	80	42.8	23.2	26.4
5	13	17.5	80.2	47.2	23.6	27
6	13	17.5	80	47.6	23.6	28
7	13	18.7	80.2	48.6	23.6	28.8
8	13	18.7	80.2	48.8	23.6	28.8
9	13	20.2	80	52.8	23.8	29
10	13	20.2	80	52.8	23.8	28.8
11	13	21.8	80.2	52.4	23.8	29.4
12	13	21.8	80.2	51.6	23.8	29.4
13	13	6.15	130.2	57.6	23.8	29.8
14	13	6.15	130	57	23.8	29.2
15	13	12.37	130.2	66.2	24.4	32.6
16	13	12.37	130.2	66.4	24.4	32.6
17	13	18.7	130	77.4	25.4	35.6
18	13	18.7	130.2	77.6	25.6	35.8
19	13	20.2	130.2	80.2	25.6	37.2
20	13	20.2	130.2	80.8	25.6	37
21	13	21.8	130.2	82	26	38.2
22	13	21.8	130	82.2	25.6	38
23	13	6.15	150.2	66.2	24	31.2
24	13	6.15	150.2	65.2	24	31.2
25	13	12.37	150.2	75.8	24.6	33
26	13	12.37	150	76.2	24.6	35.4
27	13	18.7	150.2	87.6	25.4	39.6
28	13	18.7	150	88.6	25.6	39.8
29	13	20.2	150	91	25.8	41
30	13	20.2	150.2	91.2	25.8	41
31	13	21.8	150.2	92.6	26.2	42
32	13	21.8	150.2	93.2	26	42.2

4. The Results of Investigation of Mass Transfer

Research data is processed through the following steps [14]. Relative air humidity on the output is calculated depending on velocity. In order to do that, from the heat balance equation the amount of vapor was calculated

$$G_1 = \frac{G_2\ \rho_2 \cdot C_2(\Delta t_2) - G_3 \cdot \rho_3 \cdot C_3(\Delta t_3) - Q_{ls}}{r}. \quad (13)$$

Relative humidity on output, vapor pressure on output, maximum vapor pressure in the air at the output air temperature are calculated as

$$d_{out} = d_{in} + G_1/G_2,$$

where

$$d_{in} = 0.01, \phi = p_{out}/p_{\max},$$

$$\mathrm{p_{out}} = 101325 \cdot \frac{d_{out}}{0,622 + d_{out}}, p_{\max} = f(t_{2v}, \phi = 1).$$

The correlation between ϕ and W was checked next. Air velocity was calculated from the continuity equation and flow rate. The data that reduce the Pearson correlation coefficient R were excluded.

In Figure 3 dependency of relative air humidity in the experimental unit from air velocity and input water film temperature is illustrated. Correlation is high and equals approximately $R^2 = 0{,}92$.

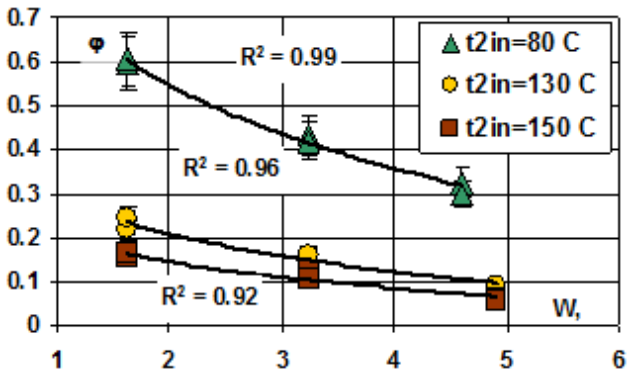

Figure 3. Dependence of output relative air humidity on air velocity and input air temperature

As we can see on Figure 3, increase in speed and temperature of air decreases its relative humidity, since air doesn't have the time to be saturated with vapor. Therefore, increase input air temperature decreases its relative humidity. Relative deflection of points from a generalized curve doesn't overcome 10%. In the future, this data will be processed.

On Figure 4 a dependency between the amount of vapor G_1 (calculated from equation (13) and velocity of air and its input temperature is shown.

Amount of vapor by convectional and diffusional transfer is calculated from analytical dependencies (8-13). Velocity of convectional vapor flow from water film equals $\upsilon = \frac{1}{\rho_2}\left(\frac{G_1}{f}\right)$. Figure 5 shows that for high velocity and temperature this parameter equals υ = 1,7 mm/s and is directly proportional to velocity W and air temperature.

From equation (11), let's calculate the scalar form of the mass content gradient of mass transfer, $\frac{d\omega_1}{dy} = \frac{\upsilon(1-\omega_1)}{D}$ and show it on Figure 6.

We'll calculate the mole part of vapor in the air (relative molar concentration) using equation $\omega_1 = \frac{\rho_1^*}{\rho^*} = \frac{\rho_1/\mu_1}{\rho/\mu} = \frac{\rho_1}{\rho}\cdot\frac{\mu}{\mu_1} \sim \rho_1$, since relative deflection ω_1 from ρ_1 doesn't exceed 11 %.

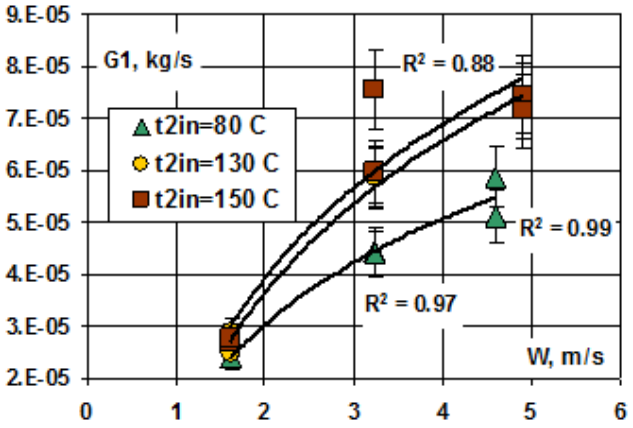

Figure 4. Dependence of the flow rate of vapour G_1 on the air velocity and input water film temperature

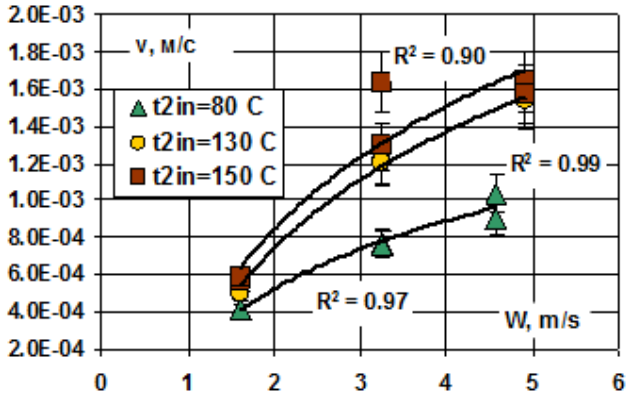

Figure 5. Dependence of velocity of convectional vapor flow υ from water film on air velocity W and input air temperature t_{2in}

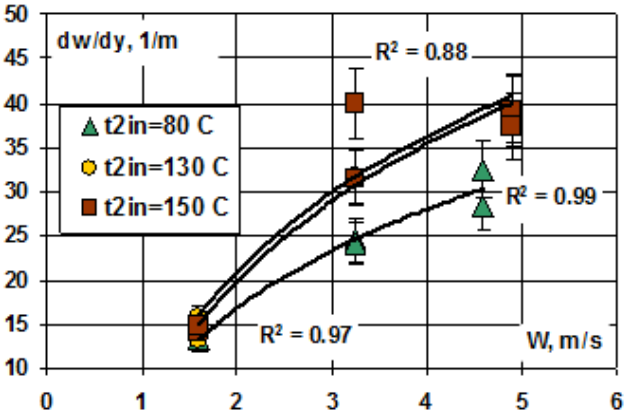

Figure 6. Dependence of mass content gradient of mass transfer on air velocity and input air temperature

Figure 6 illustrates that for high velocity and temperature this parameter reaches up to 40 1/m and is directly proportional to air velocity and its input temperature. Knowing the value of derive, shown on Figure 6, in equation (12) $\dot{m}_1 = -\rho D \frac{\partial \omega_1}{\partial y} + \rho_1 \upsilon$ we have the first term – diffusional component part of mass transfer, where $\rho \approx \rho_2$.

On Figure 7 $\rho_2 D \frac{d\omega_1}{dy}$ is shown, depending on air velocity and its input temperature. We'll calculate directly the second term $\rho_1 \upsilon$ in equation (12) that characterizes the convectional mass transfer component and show it on Figure 8. By comparing Figure 7 and Figure 8 we can see that mass transfer by diffusion is by 2 orders higher than transfer by convection, however the general dependencies remain. As seen on Figure 7 and Figure 8, calculated values are summarized by dependencies with a high value of correlation coefficient $R^2 > 0.69$ and with all this, the relative deflection of calculated values from empirical curves doesn't overcome 10%, excluding mistakes. Therefore, increase in air velocity and its input temperature leads to increase in diffusional and correlational mass transfer. But the main is the diffusional mass transfer.

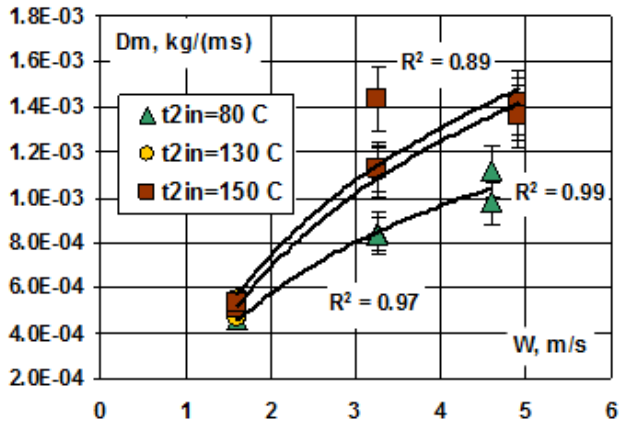

Figure 7. Dependence of diffusional mass transfer component on air velocity and input air temperature

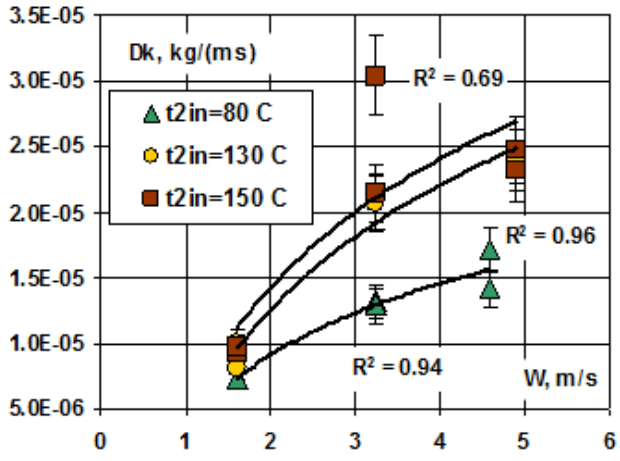

Figure 8. Dependence of convectional mass transfer component on air velocity and input air temperature

If we count that

$$\dot{m}_1 = -\rho D \frac{d\omega_1}{dy} - \frac{\rho_1}{1-\omega_1} D \frac{d\omega_1}{dy} = -\frac{\rho^2}{\rho_2} D \frac{d\omega_1}{dy},$$

then if $\rho \approx \rho_2$ – mixture density is close to air density, we have $\dot{m}_1 = -\rho D \frac{\partial \omega_1}{\partial y}$. This theoretically proves that convectional mass transfer can be neglected.

From the last equation let's define the diffusional mass transfer layer thickness in scalar form

$$\frac{1}{\partial y} = \frac{\dot{m}_1}{\partial \omega_1} \frac{1}{\rho D},$$

where $\partial \omega_1 = \omega_{1w} - \omega_{1s} = \rho_1 - \rho_{1s}$

On the other hand, its known $\beta c = \frac{\dot{m}_1}{\partial \omega_1}$. Therefore, $\beta c \frac{1}{\rho D} = \frac{1}{\partial y}$, where $\frac{1}{\rho D} = const$ – mass transfer coefficient βc is inversely proportional to the thickness of diffusional mass transfer layer.

Let's calculate the experimental value of the thickness of diffusional mass transfer layer ∂y that characterizes mass transfer coefficient.

$$\partial y = \frac{\rho_2 D}{\dot{m}_1} \partial \omega_1 = \frac{\rho_2 D}{\dot{m}_1} (\rho_1 - \rho_{1s}) \qquad (14)$$

and compare it to the theoretical, calculated form the dependency for the displacement layer thickness [13] on the base of boundary layer theory

$$\delta = 0.376 \cdot 4.64 \cdot \sqrt{\frac{\nu_2 y}{\upsilon_2}}, \qquad (15)$$

where y =1000/2 mm – average value of the tube in experimental unit.

Calculated the experimental value of the thickness of diffusional mass transfer layer (eq. 14) are shown as points on Figure 9. Figure 9 shows that experimental value ∂y grows with the increasing of input air temperature in range of 80...150 °C and decreases with the growing air velocity. However, if for temperature value of t_{2in} = 150 °C this decrease equals 0.2 mm, then for t_{2in} = 80 °C it equals 0.05 mm. The correlation coefficient R^2 >0.35 prove the existence of correlation.

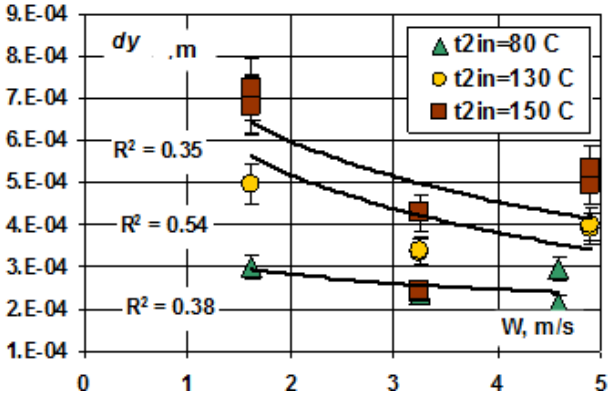

Figure 9. Dependence of the experimental value of the thickness of diffusional mass transfer layer ∂y on air velocity and input air temperature

For comparison, Figure 10 illustrates theoretical values of displacement layer thickness δ in a channel of similar diameter (eq. 15).

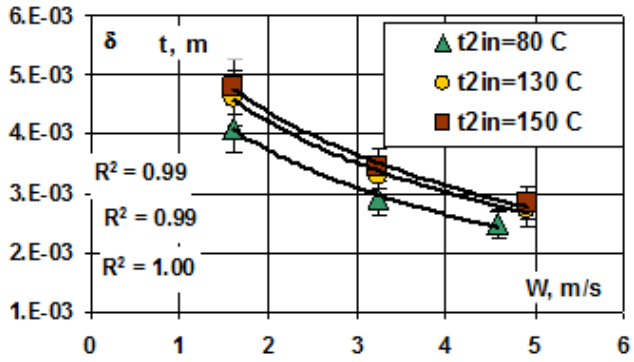

Figure 10. Dependence of theoretical values of displacement layer thickness δ on air velocity and input air temperature

Figure 10 shows that in air velocity range of 1,6-4,9 m/s theoretical values confirm experimental ones only qualitatively – decrease in theoretical value of displacement layer thickness happens while air velocity increases and input air temperature decreases. As seen on Figure 10, resulting points with a deflection of ±10% are generalized with shown curves. However, after comparing Figure 9 and Figure 10 you can see that theoretical values of displacement layer thickness δ can reach 7...8 times more than the experimental value of the thickness of diffusional mass transfer layer ∂y. This is explained by the length of the experimental unit (y =1 m), that exceeds the calming length zone y from the equation (15). This means that mass transfer process takes place in a steady flow.

Therefore let's not use displacement layer thickness as a mass transfer diffusional layer thickness if length of the work area exceeds the calming length zone.

From equation

$$\dot{m}_1 = -\rho D\left(\frac{\partial \omega_1}{\partial y}\right)_w = \beta c\left(\omega_{1\omega} - \omega_{1s}\right)$$

let's calculate mass transfer coefficient as $\beta c = \dfrac{\dot{m}_1}{\omega_{1\omega} - \omega_{1s}}$.

Figure 11 shows a dependence of experimental value of mass transfer coefficient on air velocity and input air temperatures. Upper curve characterizes mass transfer at input air temperature of 80 °C, middle one - 130 °C and the bottom one for 150 °C. Figure 11 illustrate that in temperature range 80...150 °C mass transfer coefficient βc is defined by air velocity. Increase of air velocity from W =1,6 to 4,9 m/s leads to increase of βc from 0,072 to 0,1 m/s (for t_{2in} =130 °C). Decrease in βc at input air temperature t_{2in} is increasing from 80 to 150 °C is explained by increase in heat on heating water film with the grow of t_{2in}. This leads to increase in partial pressure of vapor near the water film and decrease of the difference in partial pressures as a gradient of the mass transfer process. As seen on Figure 11, experimental data differs from empirical curves up to 10 % (excluding mistakes).

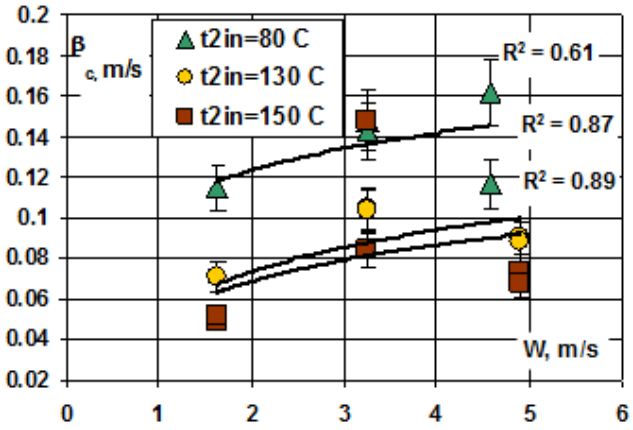

Figure 11. Dependence of experimental value of mass transfer coefficient on air velocity and input air temperature

On Figure 12 dependence of theoretically calculated mass transfer coefficient βc_t (defined from an equation $\beta c_t = \rho D / \delta_t$), from air velocity and its input temperature is shown. As seen on Figure 12, mass transfer coefficient βc_t is defined by air velocity since the influence on βc_t the input air temperature at the range 80...150 °C is not significant. For example, decrease in air temperature from 80 to 150°C leads to decrease in theoretical value of mass transfer coefficient by 20% or from 0,012 to 0,01 m/s (at air velocity W = 3,2 m/s). Comparison the values of mass transfer coefficient on Figure 11 and Figure 12 shows that the theoretical calculation confirms experimental results only qualitatively.

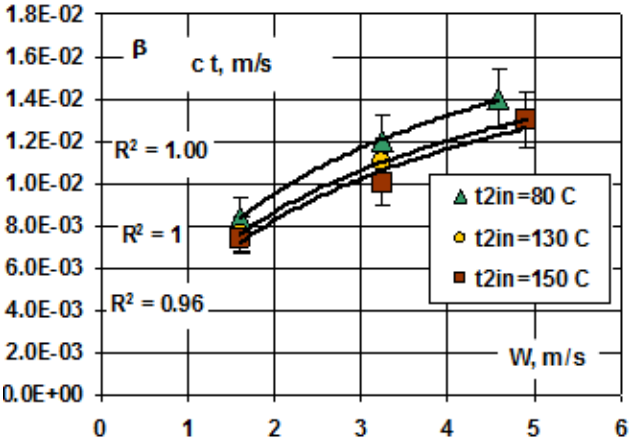

Figure 12. Dependence of theoretically calculated mass transfer coefficient on air velocity and input air temperature

But experimental value of mass transfer coefficient is 6-10 times higher than the theoretical one and the difference grows with the increasing air velocity. Therefore it's unacceptable to use displacement layer thickness as a mass transfer diffusional layer thickness when the length of work area exceeds the calming length area.

In this case we use theory of similarity for summarizing experimental data on mass transfer.

On Figure 13 summarizing of experimental data on mass transfer with using theory of similarity at high value of correlation coefficient R^2 = 0.78 is shown.

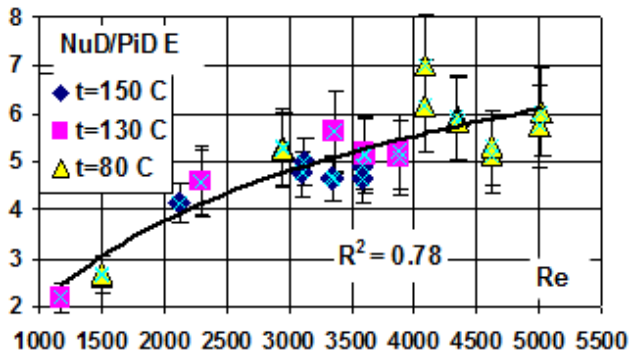

Figure 13. Empirical correlations of experimental data on mass transfer

Figure 13 shows that deflection of experimental data from the empirical curve does not exceed 15%, excluding mistakes. The selection of dimensionless criteria is based on the theory of similarity and literature review [15]. Calculated criteria equation was obtained by the least square method $Nu_D = 0,014\,\mathrm{Re}^{0,72}\,\pi_d^{-0,76}\varepsilon^{0,38}$ in range of t_{2in} =80... 150 ° C, Re = 1100…5000, π_d = 0,0027…0,028, ε = 0,029…0,053 and it summarizes experimental data.

5. Conclusions

Experimentally researched mass transfer process for steady air flow in a contacting conditioner 1 m high and ∅16,5/37 mm for input air and water film temperatures 80...150 C and 25°C shows that:

1. Diffusional mass transfer component is 6...45 times higher (depending on air velocity) than convectional mass transfer component. Therefore the latter can be neglected in calculations.

2. The theoretical values of displacement layer thickness δ_t exceeds the experimental value of the thickness of diffusional mass transfer layer δ by 7÷10 times since the calming length zone in a channel is lower than the height of the tube in experimental unit. This leads to exceeding by one order the experimental value of mass transfer coefficient βc in comparison to the theoretically calculated mass transfer coefficient βc_t using theoretical values of displacement layer thickness. Despite this, the trend of the dependence of βc from air velocity and input air temperature for theoretical and experimental coefficients was confirmed qualitatively.

3. Calculation βc for steady air flow in a channel is recommended by using the calculated criteria equation was obtained by the least square method, based on a theory of similarity. Deflection βc from the generalized equation goes up to ±15%.

List of Abbreviations

h, J/kg – specific enthalpy,
υ, m/s – velocity,
D, m^2/s – mass diffusion coefficient,
t, C – temperature,
G, kg/s – flow rate,
c, J/kg/K – heat capacity,
m, kg – mass,
d, kg/kg – absolute humidity,
W, U, m/s – air and water film velocity,
B, Pa –atmospheric pressure,
$\dot{m}$, kg/m2/s – specific flow rate,
f, m^2 – contact area,
L, m – perimeter of contact area,
Q, W – heat power,
q, W/m^2 – specific heat,
R – Pearson correlation coefficient,
Dm, kg/m^2/s – mass diffusion flow,
Dk, kg/m^2/s – mass convection flow,
V, m^3 – volume,
x, y, m – longitudinal and transverse coordinates,
p, Pa – pressure,
r, J/kg – latent heat,
α, W/m^2/K –heat transfer coefficient,
βc, m/s – mass transfer coefficient,
ν, m^2/s – kinematic viscosity,
ρ, kg/m^3 – density,
δ, m – displacement thickness,
μ – mole mass,
ϕ – relative humidity,
λ, W/m/K – thermal conductivity,
Δ – difference of input and output parameters,
χ, m – radius,
ω –mass fraction of vapour,
$Nu_D = \beta c \cdot 2R/D$ – diffusion Nusselt number,
$\mathrm{Re} = W \cdot 2R/\nu_2$ – Reynolds number,
$\pi_d = (p_w - p_s)/B$ – dimensionless complex,
$\varepsilon = p_w/B$ – dimensionless complex.

Indexes:
1, 2, 3 – vapour, air and water film respectively,
s, w – humid air in stream and near the water film,
ls – loss,
t – theoretic,
wb – wet-bulb conditions,
in, out – input and output respectively.

References

[1] Qureshi B.A., Zubair S.M. "A complete model of wet cooling towers with fouling in fills," *Applied Thermal Engineering*, 26, 1982-1989. 2006.

[2] Naphon P. "Study on the heat transfer characteristics of an evaporative cooling tower," *International Communications in Heat and Mass Transfer*, 32, 1066-1074. 2005.

[3] Alekseev V.P, Yssledovanye protsessov teplo- y massoobmena v apparatakh kholodyl'nikh ustanovok s rehulyarnimy nasadkamy, Ph.D. thesis in Engineering Science, Odesa, 1969, 246.

[4] Heorhalina O.R, Modelyuvannya ta optymizatsiya plivkovykh okholodzhuvachiv Ph.D. thesis in Engineering Science. Kyiv polytechnical institute, Odesa, 2004, 185.

[5] Heshev P.Y., Kovalev O.P., Tsvelodub O.Yu., Yakubovskyy Yu.V. "Teplomassoobmen pry kontakte horyacheho haza so stekayushchey plenkoy zhydkosty", *YFZh*, 46 (3), 428-432. 1984.

[6] Tuz V.E, Kontaktniy teplomassoobmenniy apparat s porystoy nasadkoy dlya toplyvnoy systemi promishlennoy gas turbine, Ph.D. thesis in Engineering Science, Kyiv, 1989, 200.

[7] Petruchyk A.Y., Fysenko S.P. “Matematycheskoe modelyrovanye ysparytel'noho okhlazhdenyya plenok vodi v hradyrnyakh,” *YFZh*, 72 (1), 43-49. 1999.

[8] Antonyk V.V., Petruchyk A.Y., Solodukhyn A.D., Stolovych N.N., Fysenko S.P. “Teplomassoobmen pry ysparytel'nom okhlazhdenyy plenok vodi na dvukh vertykal'nikh plastynakh” *in Trudi IV Mynskoho Mezhdunarodnoho foruma po teplomassoobmenu*, Minsk, 314-325. 2000.

[9] Chou Y., Ruey-Jen Y. “The evaporation of a saturated porous layer inside an inclined airflow channel” *International Journal of Heat and Fluid Flow*, 28, 407-417. 2007.

[10] Saouli S., Boumaza M., Settou N., Aiboud-Saoili S., Daguenet M. “Numerical study of the evaporation of a falling Ostwaldian film along an inclined flat plate into a laminar stream of humid air”, *in 4th International Conference on heat Transfer, Fluid Mechanics and Thermodynamics (HEFAT 2005)*, Cairo, Egypt, 19-22.

[11] Feddaoui M., Meftah H., Mir A. “The numerical computation of the evaporative cooling of falling water film in turbulent mixed convection inside a vertical tube,” *International Communications in Heat and Mass Transfer*, 33, 917-927. 2006.

[12] Zhang H., Tao W., He Y., Zhang W. “Numerical study of liquid film cooling in a rocket combustion chamber,” *International Journal of Heat and Mass Transfer*, 49, 349-358. 2006.

[13] Schlichting H, BoundaryLayer Theory, McGraw-Hill, 1960, 510.

[14] Kuzmenko I., Prokopets R. “Experimental and theoretical investigation of mass transfer in a cooling tower,” *Energetica*, 1, 27-35. 2014.

[15] Isachenko V.P., Osipova V.A., Sukomel A.S., Heat exchange, Aris, 2014, 416.